Experimental and theoretical study of double-electron capture in collisions of slow $C^{4+}(1s^2\ ^1S)$ with $He(1s^2\ ^1S)$

M. Hoshino,[1,2,*] L. Pichl,[3,†] Y. Kanai,[1] Y. Nakai,[1,‡] M. Kitajima,[2,§] M. Kimura,[4] Y. Li,[5] H.-P. Liebermann,[5] R. J. Buenker,[5] H. Tanaka,[2] and Y. Yamazaki[1,6]

[1]*Atomic Physics Laboratory, RIKEN, Saitama 351-0198, Japan*
[2]*Department of Physics, Sophia University, Tokyo 102-8554, Japan*
[3]*International Christian University, Tokyo 181-8585, Japan*
[4]*Graduate School of Science, Kyushu Univeristy, Fukuoka 812-8581, Japan*
[5]*Fachbereich C-Mathematik und Naturwissenschaften, Bergishes Universität Wuppertal, 42119 Wuppertal, Germany*
[6]*Institute of Physics, University of Tokyo, Tokyo 153-8902, Japan*

(Received 4 November 2006; published 22 January 2007)

The doubly differential cross sections (DDCS) of double electron capture in collisions of slow C^{4+} with He were measured in the energy range of 240, 320, and 440 eV (in laboratory frame) using a crossed-beam apparatus and represented as a two-dimensional contour map. The double-electron capture into the $C^{2+}(1s^2\ 2s^2\ ^1S)$ state was found to be dominant in the present energy range. The Stückelberg oscillation structures, which result from interference among two different paths on the interaction potential curves, were clearly observed in the DDCS at the present low impact energies. The differential cross sections were also calculated in an *ab initio* molecular orbital framework for $(CHe)^{4+}$, and show a good agreement with the present experimental results.

DOI: 10.1103/PhysRevA.75.012716 PACS number(s): 34.70.+e

I. INTRODUCTION

A number of electron capture processes in collisions of slow highly charged ions (HCIs) with atomic targets have been investigated experimentally and theoretically not only for interest in atomic collision physics [1] but also for their importance in fields such as astrophysics [2] or fusion plasma diagnostics [3]. The state-selective angular differential cross sections (DCS) of the electron capture in HCI-atom collision are closely related to the impact-parameter dependence on classical trajectories of the collision systems and provide useful information on the level crossings, the strength of the coupling, and the shape of the interaction potential curves directly, especially in the low energy region [4,5]. Several examples of electron capture processes in such systems were reported in the review of Barat and Roncin [6].

The C^{4+}-He system has been experimentally studied as a prototype for the collision of a He-like ion with the He atom. This system is the simplest case that incorporates Coulomb potentials of different charge states in the product channels which lead to single and double electron capture from He. Several groups have investigated this system from the viewpoint of both experiment and theory in the low energy region, especially, since double electron capture was found to be the dominant channel in the pioneering study by Crandall *et al.* [7,8]. Okuno *et al.* found that only the ground state of C^{2+} was populated in the double electron capture as in Eq. (1) by the energy gain spectroscopy at impact energy of 3.7 keV [9],

$$C^{4+} + He(1s^2\ ^1S) \rightarrow C^{2+}(2s^2\ ^1S) + He^{2+}. \quad (1)$$

This was also shown in the theoretical work of Kimura and Olson [10].

Cederquist *et al.* have found an oscillation pattern in the energy gain spectrum of C^{2+} at 500 eV, which was a projection of the angular distribution of scattered C^{2+} to the energy gain via a kinematic relation between the projectile scattering angle and energy gain [11]. This oscillation was attributed to the Stückelberg oscillations, which result from the interference among two different collision paths on the interaction potential energy curves, based on a theoretical calculation of DCS using model potential curves obtained semiempirically [12,13]. Only the initial C^{4+}-He channel and the final $C^{2+}(2s^2)$-He^{2+} channel were considered and a direct coupling between these channels was incorporated in this model. The potential curves were represented by polarization and Coulomb-type diabatic potentials with position dependent effective charges. The coupling between the diabatic states was estimated from the analytical formula of Grozdanov and Janev [14]. DCS calculations based on the two-state semiempirical representation also successfully reproduced the Stückelberg oscillations observed clearly in the angular dependence of double electron capture at 1520 eV of Cocke *et al.* referred in Refs. [12,13]. Therefore, the semiempirical two-state model were relied upon as an adequate representation at low energies. However, it was found that the two-state semiempirical model fails to reproduce the angular distribution C^{2+} obtained at very low energy of 400 eV by Keller *et al.* [15]. At higher energies, Barat *et al.* [16] have measured the state-selective DCS at 6.0 and 9.6 keV. Since the cross sections of single electron capture start to

*Electronic address: masami-h@sophia.ac.jp
†Electronic address: lukas@icu.ac.jp
‡Present address: Radioactive Isotope Physics Laboratory, RIKEN, Saitama 351-0198, Japan
§Present address: Department of Chemistry, Tokyo Institute of Technology, Tokyo 152-8551, Japan

 ©2007 The American Physical Society

substantially increase at these energies, the two-state model breaks down. Therefore, Barat *et al.* proposed a four-state model including the single electron capture channels which reproduces their experimental results at 6.0 and 9.6 keV well [16]. As was the case of the two-state model, this four-state model did not reproduce the results of Keller *et al.* [15].

Recently, we have presented the state selective measurements of angular distribution of double electron capture in C^{4+}-He collisions at 270 and 470 eV [17], and compared with the calculated DCS based on the model potential of Boyed *et al.* [18], which were obtained through the modification of the potential of Bárány *et al.* [12,13] by deducing parameters of an inverse problem. A clear discrepancy between the experimental and calculated results was found, especially at the very low energy at 270 eV. We have also presented improved measurements with a two-dimensional (2D) contour map on the energy gain—scattering angle plane at 400 eV, which showed the Stückelberg oscillations clearly [19]. The 2D contour map provides state-resolved information resolved better than the conventional energy gain spectra or angular distribution representation. The results obtained at 400 eV [19] appeared to be consistent with the results of our previous work at 270 and 470 eV [17]. The oscillation periods observed on the 2D contour map were in a good agreement with the results of Keller *et al.* [15], but the peak position were slightly shifted. Also the angular dependence of the peak intensities at larger angles did not match.

More recently, we have reported a calculation of differential cross sections of double electron capture in C^{4+}-He collisions based on the full *ab initio* treatment of electronic states [20]. The calculated results showed a good agreement with our previous measurements at 400 eV. It was also found that the detailed theoretical treatment of the potential curves and the couplings among the reaction channels becomes much more important to reproduce the experimental DCS in the lower energy region than was expected before. However, as the Stückelberg oscillations in our angular spectra at 270 and 470 eV were unresolved, the experiment did not provide a stringent test for the calculated cross sections at 270 and 470 eV. Since the Stückelberg oscillation becomes quite sensitive to the details of potential curves, it is worthwhile to observe and clarify the oscillation patterns in the lower energy region. Therefore, we extended the detailed measurements based on the 2D contour map approach toward lower collision energy.

In this paper, we present the state-selective angular distribution measurements of C^{2+} in $C^{4+}(1s^2 {}^1S)$-He collisions at 240, 320, and 440 eV with the 2D contour map on the energy gain—scattering angle plane. A close-coupling calculation of this collision process using 10-channel *ab initio* adiabatic potential energy curves and their nonadiabatic coupling matrix elements is also presented and compared with the experimental results. The resultant set of experimental and theoretical data directly elucidates the dynamics of the collision process.

II. EXPERIMENTS

The experiment was carried out at the slow highly charged ion-beam facility in RIKEN [21]. The experimental setup has been described before [19,22]. Briefly, the $C^{4+}(1s^2 {}^1S)$ ion beam from the 14.5 GHz Caprice-type electron cyclotron resonance ion source was extracted and transported at around 8.0 keV to the collision chamber, which contains a crossed-beam apparatus. The ion beam was decelerated down to 0.8 keV just before the collision chamber by the deceleration lens system in the beamline. The crossed-beam apparatus consists of an ion-energy selector, an effusive nozzle, a scattered ion analyzer, and a beam profile monitor. The ion beam was decelerated to the desired energy and energy-selected by the ion-energy selector. Target He gas was introduced by the multicapillary array nozzle perpendicular to the scattering plane. Scattered ions were energy analyzed by a hemispherical analyzer, which can be rotated from $-15°$ to $+60°$ with respect to the beam direction.

Two-dimensional (2D) contour maps of scattered ion intensities were constructed with respect to the kinetic energy difference before and after collisions, ΔE, and the scattering angle of the projectile in the laboratory system, θ_{lab} [19]. The correction for the change of scattering geometry with scattering angle, i.e., the effective path length correction [23] has been estimated from the comparison of the angular distribution of the He^+-He elastic scattering measured by our setup with the angular differential cross sections published in Ref. [24]. The kinematic relation of scattered ion between ΔE and θ_{lab} was derived from the energy and momentum conservation law for inelastic two-body collisions [9], which includes the inelastic energy transfer Q. Since the initial energy is well defined, one can specify the final state after a charge exchanging collision of HCI with an atom by measuring the ΔE and θ_{lab}. Typical energy and angular resolutions are estimated as $\delta E/E \sim 1/150$ and $\pm 1.0°$, respectively, where δE and E are the energy spread and the impact energy.

III. THEORY

We explain our theoretical method briefly, since it was already described before in Ref. [20]. In order to obtain the potential curves of the C^{4+}-He system, we have carried out *ab initio* configuration interaction calculations by using an extended version of the multireference single- and double-excitation MRD-CI programs [25,26]. The correlation consistent polarized valence quadruple zeta, cc-pVQZ Gaussian basis [27] was employed for the C and He atoms. A selection threshold of 10^{-9} hartree was used to select the configuration wave functions of which the electronic wave functions are composed. Potential energy curves for nine low-energy charge transfer states significantly coupled to the initial channel were computed for the internuclear distance R between 0.8 and 110 atomic units. The higher lying roots are important for the representation of the flat initial collision channel, as well as the series of its crossings with the single- and double-electron capture states, all of which exhibit Coulomb repulsion asymptotic behavior. In the region of internuclear distances above 25 a.u., all curve crossings were found to be strictly diabatic. The corresponding nonadiabatic couplings among all states involved were evaluated by using a numerical differentiation method [28].

The de Broglie wave length of the projectile at the lowest energy considered in the present work is 1.5×10^{-3}a.u., due

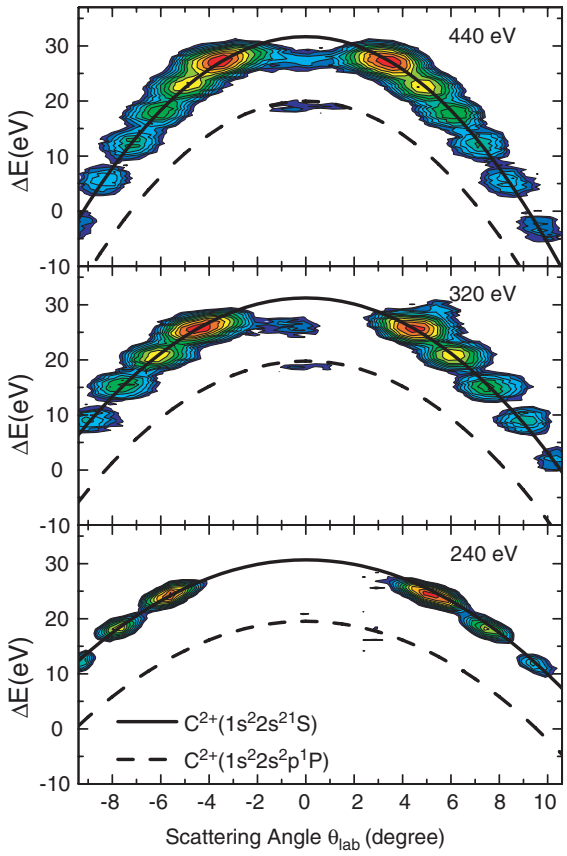

FIG. 1. (Color online) DDCSs of scattered C^{2+} ions in C^{4+}-He collisions at 240, 320, and 440 eV. Solid and broken curves indicate the expected ΔE as a function of the scattering angle θ_{lab} for the final states specified by $Q=20.7$ and 33.4 eV, respectively.

to the large mass of the C^{4+} projectile, and much below the characteristic distance of the potential matrix. Therefore, in the calculation of differential cross sections, we applied the eikonal approximation to solving the coupled equations for state-dependent transition amplitude, $c_{f,i}(b,z)$. The diabatic curves of the initial collision state, double-capture state, and their couplings were obtained by the procedure of Heil [29] and compared to available semiempirical models in a recent paper [20]. The semi-classical formulation of the coupled equations for the transition amplitudes is given in detail in references[30,31]. The cross section follows from the diffraction integral of the transition amplitude,

$$\frac{d\sigma}{d\Omega}(\theta) = (mv)^2 \left| \int_0^\infty J_0(\eta b) c_{f,i}(b;\infty) b db \right|, \qquad (2)$$

where m is the reduced mass, v is the relative collision velocity, J_0 is the Bessel function, and $\eta=2mv\sin(\theta/2)$ [30]. To calculate the diffraction integral in Eq. (2), we employed a grid of 10 000 impact parameter points.

IV. EXPERIMENTAL RESULTS

A. Doubly differential cross sections

Figure 1 shows the relative doubly differential cross sections (DDCS) with respect to the energy gain and the scattering angle of C^{2+} produced in charge-transfer collisions of C^{4+} with He at impact energy of 240, 320, and 440 eV. In the 2D contour map, signals from each of the final states of the electron capture align on the curve of kinematic relation specified by the Q value. In Fig. 1, solid and broken curves show the kinematical relations between ΔE and θ_{lab} for the final electronic states of $C^{2+}(1s^2 2s^2\ ^1S)$ and $C^{2+}(1s^2 2s 2p\ ^1P)$, respectively. Scattering intensity of C^{3+} from single electron capture were one order smaller than those of the double electron capture at present impact energies, which is consistent with the previous measurements [9]. Figure 1 shows that the formation of the $C^{2+}(1s^2 2s^2\ ^1S)$ state dominates the double electron capture. Only a very small contribution to the $C^{2+}(1s^2 2s 2p\ ^1P)$ state formation was observed at forward scattering at 440 eV.

The 2D representation enables us to clearly resolve the oscillation patterns which correspond to the Stückelberg oscillations in the DDCS, due to the high resolution in ΔE. The position of the first forward peak, which has the largest intensity, shifts to the larger scattering angle with decreasing the impact energy. The oscillation period increases with decreasing the impact energy. The 2D contour map of 440 eV in the present measurements resembles to that of our previous results obtained at 400 eV [19]. Judging from the impact energy dependencies of the position of the first peak and the oscillation period observed at 240, 320, and 440 eV, present measurements show consistent results with our previous ones obtained at 400 eV [19]. Although our previous data [17] at 270 and 470 eV had insufficient resolution allowing only for the position of the most forward peak to be recognized, the positions of the most forward peak for 240 and 440 eV are almost the same as those for 270 and 470 eV [17], respectively.

B. Impact energy dependence of oscillation structure

Figure 2 shows the impact energy dependence of the Θ_1, Θ_2, and Θ_3, which are the angles in the center-of-mass (CM) system of the first, second, and third peak in the oscillation structures. Θ_{TH} is the threshold angle at the forward scattering in the DDCS. Note that the Θ_{TH} is somewhat uncertain because it is not possible to determine it accurately due to experimental resolution. Previous measurements at energies of 1520 eV by Bárány*et al.* [12,13], 6.0 and 9.6 keV by Barat *et al.* [16] are also plotted in Fig. 2. Thin solid, thick solid, broken, and dashed curves correspond to the fitting function for each peak positions. The fitting function is given by,

$$\sin\Theta_{\text{CM}} = \frac{2E_{\text{CM}}^{-a}}{\sqrt{(2E_{\text{CM}}^{-a})^2 + b^2}}, \qquad (3)$$

where Θ_{CM} and E_{CM} are the scattering angle and impact energy in the center-of-mass system, respectively; atomic units are used through this section unless indicated. The a and b are adjustable parameters. When $a=1.00$, this function corresponds to the Rutherford formula for classical trajectory of a half collision in a simple Coulomb interaction potential,

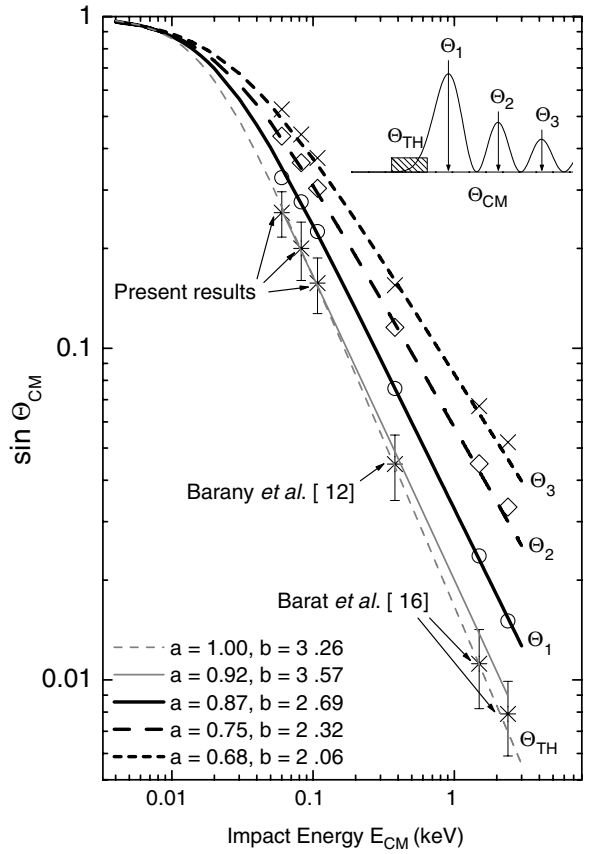

FIG. 2. Impact energy dependence of the peak positions in the oscillation structures. The Θ_1, Θ_2, and Θ_3 correspond to the first, second, and third peak angles, whereas Θ_{TH} is the threshold of the differential cross sections. See text for details.

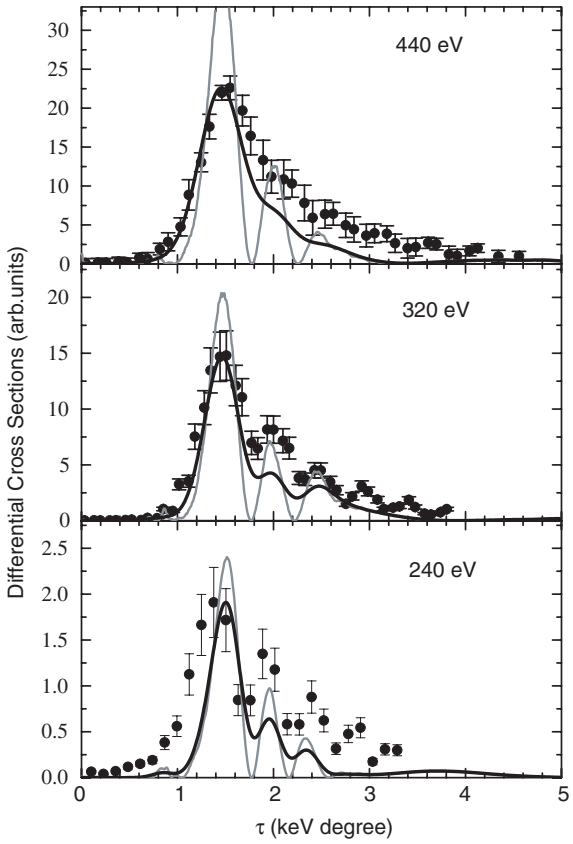

FIG. 3. (Color online) Comparison between experimental angular differential cross sections and calculations at energies of 240, 320, and 440 eV. (●); measured experimental DCS. Thick and thin lines; calculations convoluted with the angular resolution of experimental apparatus and nonconvoluted results, respectively.

$4/r$, i.e., Coulomb potential between a pair of doubly charged positive ions. Parameter b corresponds to the impact parameter. The value of $b=3.26$ a.u. corresponds to a crossing radius when a flat potential for the initial channel and a Coulomb potential for the final channel (C^{2+}-He^{2+}) are assumed. The fitted curve for Θ_{TH} yields $(a,b)=(0.92,3.57)$, which are close values compared to the Rutherford formula, $(a,b)=(1.00,3.26)$. The other values are found to decrease as the angle position becomes larger.

Under the assumption of forward scattering and applicability of Coulomb potential for the collision, $\Theta_{CM}E_{CM}$ is almost constant. However, the present experimental results show that such an approximation breaks down at low impact energy, certainly below 400 eV in the laboratory system. This effect for Θ_3 becomes more noticeable than for Θ_1 because the impact parameter corresponding to Θ_3 is smaller than the one for Θ_1. This indicates that the simplification of potential curves by the initial flat potential and the final Coulomb potential becomes more insufficient at smaller nuclear distance.

V. COMPARISON BETWEEN EXPERIMENT AND CALCULATION

Figure 3 shows the experimental DCSs for double-electron capture into $C^{2+}(1s^22s^2\ ^1S)$ at 240, 320, and 440 eV, which are obtained from 2D contour maps. The calculated DCSs are also shown in Fig. 3. Both experimental and calculated DCSs are plotted as a function of reduced scattering angle $\tau(=\theta_{lab}E_{lab})$ (keV degree). The calculated DCSs (thick line) were convoluted with the angular resolution of present experimental apparatus and normalized to the experimental DCS at the most forward peak. The Stückelberg oscillations are clearly resolved at lower energies in the present experimental DCS. Since the oscillation period becomes small, minima of the Stückelberg oscillations become shallow at the highest energy. However, the oscillatory structures are still visible. The experimental results show a slight shift of the peak position toward larger τ with increasing the impact energy. The peak position of the calculated results is rather static in this energy region, located at $\tau\sim 1.46$ keV degree. The oscillation period in the reduced angle slightly increases with the impact energy as shown in Fig. 3. This dependence of the oscillation period on the impact energy is reproduced by our calculation. The agreement of the present results is much better than the one obtained from the previous semiempirical model, and the accuracy of the present *ab initio* calculation can thus be confirmed from the above comparison at 240, 320, and 440 eV.

As was discussed in Ref. [20], the *ab initio* calculation confirms, in accordance with previous semiempirical models,

that the CHe^{4+} collision system can be described by two electronic states with electronic configurations corresponding to the initial and main double electron capture states at low energies. Thus, the two-state semiempirical model includes a part of the essential features of the reaction mechanism derived from the present *ab initio* calculation. The semiempirical model based on the polarization and Coulomb-type diabatic potentials with the position dependent effective charges, however, does not describe the molecular ion sufficiently at small internuclear distances, which results in a displacement of the avoided crossing by about 0.5 a.u. from the exact location, and a steeper slope of the potential energy curves at the avoided crossing. The process of double electron capture is driven by a broad nonadiabatic coupling peak, which corresponds to a delocalized transition between the two asymptotic states, and differs from the approximate models based on the coupling in Ref. [14].

The details of the potential curve shapes, and the size of the transition region are decisive at lower energies, where the interplay of accurate transition probabilities and transition phases is crucial for the differential cross section. We therefore conclude that in the present low energy region, although the semiempirical models based on the Coulomb-type potential models could interpret experimental cross sections with adjusted effective charges, they fail to reproduce the electronic structure of the transition molecular ion, and correspondingly the delocalized dynamics of electron capture at lower energies.

VI. CONCLUSION

We have measured the relative doubly differential cross sections (DDCS) with respect to the energy gain and the scattering angle of C^{2+} produced in the double electron capture in the collisions of C^{4+} ions with He for projectile energies 240, 320, and 440 eV in the laboratory system. The two-dimensional (2D) contour map on the energy gain and scattering angle plane enabled us to resolve the Stückelberg oscillations clearly. The experimental results showed that the double electron capture into the $C^{2+}(2s^2\ ^1S)$ state dominates below 440 eV. Present results at 240, 320, and 440 eV were consistent with our previous results obtained at 400 eV [19]; this applies also to our earlier measurements at 270 and 470 eV [17], taking into account the insufficient angular resolution of the previous data. *Ab initio* potential curves and couplings have been obtained in order to calculate the theoretical DCS for the present system. The analysis of *ab initio* potential curves and couplings confirms the applicability of a two-state model, although a number of adiabatic states are necessary to represent the initial and final diabatic potentials for large internuclear distances. The agreement of the present experimental and calculated results at 240, 320, and 440 eV is considered to be very good, which confirms the accuracy of the present *ab initio* calculation. It is also confirmed that DCS is more sensitive to the potential curves and couplings in the lower energy region and hence DDCS measurements with 2D representation of electron capture at low energy are useful for the study of the physics in HCI-atom collisions.

ACKNOWLEDGMENTS

The authors would like to thank Yoh Itoh at Josai University for his kind help in the construction of our apparatus by crossed-beam method. A part of our apparatus was constructed by Special Coordination Funds for Promoting Science and Technology. Two of authors (M.H. and M.K.) had been supported by Special Postdoctoral Researchers Program at RIKEN. Partial support by the Academic Frontier Program of MEXT (L.P.) and Grant No. Bu 450/7-3 from the Deutsche Forschungsgemeinschaft (H.P.L. and R.J.B.) is also acknowledged.

[1] R. K. Janev and H. P. Winter, Phys. Rep. **117**, 265 (1985).
[2] C. M. Lisse, K. Dennerl, J. Englhauser, M. Harden, F. E. Marshall, M. J. Mumma, R. Petre, J. P. Pye, M. J. Ricketts, J. Schmitt, J. Trümper, and R. G. West, Science **274**, 205 (1996).
[3] J. D. Gillaspy, J. Phys. B **34**, R93 (2001).
[4] H. Laurent, M. Barat, M. N. Gaboriaud, L. Guillemot, and P. Roncin, J. Phys. B **20**, 6581 (1987).
[5] Y. Itoh, J. Phys. B **35**, 3217 (2002).
[6] M. Barat and P. Roncin, J. Phys. B **25**, 2205 (1992).
[7] D. H. Crandall, R. E. Olson, E. J. Shipsey, and J. C. Browne, Phys. Rev. Lett. **36**, 858 (1976).
[8] D. H. Crandall, Phys. Rev. A **16**, 958 (1977).
[9] K. Okuno, H. Tawara, T. Iwai, Y. Kaneko, M. Kimura, N. Kobayashi, A. Matsumoto, S. Ohtani, S. Takagi, and S. Tsurubuchi, Phys. Rev. A **28**, 127 (1983).
[10] M. Kimura and R. E. Olson, J. Phys. B **17**, L713 (1984).
[11] H. Cederquist, L. H. Anderson, A. Bárány, P. Hvelplund, H. Knudsen, E. H. Nielsen, J. O. K. Pedersen, and J. Sorensen, J. Phys. B **18**, 3951 (1985).
[12] A. Bárány, H. Danared, H. Cederquist, P. Hvelplund, J. O. K. Pedersen, C. L. Cocke, L. N. Tunnell, W. Waggoner, and J. P. Giese, J. Phys. B **19**, L427 (1986).
[13] H. Danared and A. Bárány, J. Phys. B **19**, 3109 (1986).
[14] T. P. Grozdanov and R. K. Janev, J. Phys. B **13**, 3431 (1980).
[15] N. Keller, L. R. Andersson, R. D. Miller, M. Westerlind, S. B. Elston, I. A. Sellin, C. Biedermann, and H. Cederquist, Phys. Rev. A **48**, 3684 (1993).
[16] M. Barat, P. Roncin, L. Guillemot, M. N. Gaboriaud, and H. Laurent, J. Phys. B **23**, 2811 (1990).
[17] M. Hoshino, M. Kitajima, Y. Kanai, Y. Nakai, H. Tanaka, and Y. Yamazaki, Phys. Scr., T **92**, 339 (2001).
[18] R. Boyd, T. S. Ho, and H. Rabitz, J. Chem. Phys. **106**, 6548 (1997).
[19] M. Hoshino, Y. Kanai, F. Mallet, Y. Nakai, M. Kitajima, H. Tanaka, and Y. Yamazaki, Nucl. Instrum. Methods Phys. Res. B **205**, 568 (2003).

[20] L. Pichl, R. Suzuki, M. Kimura, Y. Li, R. J. Buenker, M. Hoshino, and Y. Yamazaki, Eur. Phys. J. D **38**, 59 (2006).
[21] Y. kanai, D. Dumitriu, Y. Iwai, T. Kambara, T. M. Kojima, A. Mohri, Y. Morishita, Y. Nakai, H. Oyama, N. Ohshima, and Y. Yamazaki, Phys. Scr., T **92**, 467 (2001).
[22] M. Kitajima, Y. Nakai, Y. Kanai, Y. Yamazaki, and Y. Itoh, Phys. Scr., T **80**, 377 (1999).
[23] R. T. Brinkmann and S. Trajmar, J. Phys. E **14**, 245 (1981).
[24] D. C. Lorents and W. Aberth, Phys. Rev. **139**, A1017 (1965).
[25] R. J. Buenker, *Proceedings of the Workshop on Quantum Chemistry and Molecular Physics*, edited by P. G. Burton (University of Wollongong Press, Wollongong, 1980) 1.5.1; R. J. Buenker, *Current Aspects of Quantum Chemistry*, edited by R. Carbo (Elsevier, Amsterdam, 1982) 81; R. J. Buenker and R. A. Philips, J. Mol. Struct. **123**, 291 (1985).
[26] S. Krebs and R. J. Buenker, J. Chem. Phys. **103**, 5613 (1995).
[27] T. H. Dunning, Jr., J. Chem. Phys. **90**, 1007 (1989).
[28] G. Hirsch, P. J. Bruna, R. J. Buenker, and S. D. Peyerimhoff, Chem. Phys. **45**, 335 (1980).
[29] T. G. Heil, S. E. Butler, and A. Dalgarno, Phys. Rev. A **23**, 1100 (1981).
[30] W. Fritsch and C. D. Lin, Phys. Rev. A **54**, 4931 (1996).
[31] M. Kimura and N. F. Lane, Adv. At., Mol., Opt. Phys. **26**, 79 (1989).